THE CURVELET TRANSFORM FOR IMAGE FUSION

Myungjin Choi, Rae Young Kim, Myeong-Ryong NAM, and Hong Oh Kim

***Abstract*— The fusion of high-spectral/low-spatial resolution multispectral and low-spectral/high-spatial resolution panchromatic satellite images is a very useful technique in various applications of remote sensing. Recently, some studies showed that a wavelet-based image fusion method provides high quality spectral content in fused images. However, most wavelet-based methods yield fused results with spatial resolution that is less than that obtained via the Brovey, IHS, and PCA fusion methods. In this paper, we introduce a new method based on a curvelet transform, which represents edges better than wavelets. Since edges play a fundamental role in image representation, one effective means to enhance spatial resolution is to enhance the edges. The curvelet-based image fusion method provides richer information in the spatial and spectral domains simultaneously. We performed Landsat ETM+ image fusion and found that the proposed method provides optimum fusion results.**

***Index Terms*— Image Fusion, Multiresolution analysis, Landsat ETM+ image, Wavelet transform, Curvelet transform.**

I. INTRODUCTION

IN MANY remote sensing and mapping applications, the fusion of multispectral and panchromatic images is a very important issue. In this regard, in the field of satellite image classification, the quality of the image classifier is affected by the fused image's quality. To date, many image fusion techniques and software tools have been developed. The well-known methods include the Brovey, the IHS (Intensity, Hue, Saturation) colour model, the PCA (Principal Components Analysis) method, and the wavelet based method [1]. Assessment of the quality of fused images is another important issue. Wald et al. proposed an approach utilizing criteria that can be employed in the evaluation of the spectral quality of fused satellite images [2].

If the objective of image fusion is to construct synthetic images that are closer to reality, then the Brovey, IHS, and PCA fusion methods are satisfactory [1]. However, one limitation of these methods is some distortion of spectral characteristics in the original multispectral images. Recently, developments in wavelet analysis have provided a potential solution to this problem. Nunez et al. developed an approach to fuse a high-resolution panchromatic image with a low-resolution multispectral image based on wavelet decomposition [3]. Ranchin and Wald designed the ARSIS concept for fusing high spatial and spectral resolution images based on a multiresolution analysis of a two-band wavelet transformation.

The wavelet-based image fusion method provides high spectral quality in fused satellite images. However, fused images by wavelets have much less spatial information than those by the Brovey, IHS, and PCA methods. In many remote sensing applications, the spatial information of a fused image is as an important factor as the spectral information. In other words, it is necessary to develop an advanced image fusion method so that fused images have the same spectral resolution as multispectral images and the same spatial resolution as a panchromatic image with minimal artifacts.

Recently, other multi-scale systems have been developed, including ridgelets and curvelets [4]–[7]. These approaches are very different from wavelet-like systems. Curvelets and ridgelets take the form of basis elements, which exhibit very high directional sensitivity and are highly anisotropic. Therefore, the curvelet transform represents edges better than wavelets, and is well-suited for multiscale edge enhancement [7].

In this paper, we introduce a new image fusion method based on a curvelet transform. The fused image using the curvelet-based image fusion method yields almost the same detail as the original panchromatic image, because curvelets represent edges better than wavelets. It also gives the same colour as the original multispectral images, because we use the wavelet-based image fusion method in our algorithm. As such, this new method is an optimum method for image fusion. In this study we develop a new approach for fusing Lansat ETM+ panchromatic and multispectral images based on the curvelet transform.

The remainder of this paper is organized as follows. The next section describes the theoretical basis of the ridgelets and curvelets . A new image fusion approach for Lansat ETM+ panchromatic and multispectral images based on the curvelet transform is subsequently presented.

This is followed by a discussion of the image fusing experiments. Next, the experimental results are analysed. Finally, the proposed method is compared with previous methods developed for image fusion, including the wavelet method and the IHS method.

The first, second and fourth authors were supported by KRF-2002-070-C0 0004.

M.-J. Choi is with SaTReC, KAIST, 373-1, Guseong-dong, Yuseong-gu, Daej eon, 305-701, Republic of KOREA (email:prime@satrec.kaist.ac.kr).

R.Y.Kim is with Division of Applied Mathematics, KAIST, 373-1, Guseong -dong, Yuseong-gu, Daejeon, 305-701, Republic of KOREA (email:rykim@amath.kaist.ac.kr).

M.-R. NAM is with SaTReC, KAIST, 373-1, Guseong-dong, Yuseong-gu, Daeje on, 305-701, Republic of KOREA (email:nam@satrec.kaist.ac.kr).

H.O.Kim is with Division of Applied Mathematics, KAIST, 373-1, Guseong- dong, Yuseong-gu, Daejeon, 305-701, Republic of KOREA (email:hkim@amath.kaist.ac.kr).

II. Ridgelet and curvelet transforms

In this section, we review the theory of ridgelet and curvelet transforms, presented in [5]–[10], which are used in the subsequent sections.

A. Continuous ridgelet transform

Let ψ be in $L^2(\mathbb{R})$ with sufficient decay and satisfying the admissibility condition,

$$K_\psi := \int \frac{|\hat{\psi}(\xi)|^2}{|\xi|^2} d\xi < \infty,$$

In this paper, we adopt Meyer wavelet ψ, which has high smoothness and a compact support in the frequency domain. We refer to [11], [12] for the definition and the basic properties of Meyer wavelet. We will suppose that ψ is normalized so that $K_\psi = 1$.

For each $a > 0$, $b \in \mathbb{R}$, and $\theta \in [0, 2\pi]$, ridgelet basis functions are defined by

$$\psi_{a,b,\theta}(x) := a^{-1/2}\psi((x_1 \cos\theta + x_2 \sin\theta - b)/a).$$

The Radon transform for $f \in L^2(\mathbb{R}^2)$ is given by

$$Rf(\theta, t) = \int f(x_1, x_2)\delta(x_1 \cos\theta + x_2 \sin\theta - t)dx_1 dx_2,$$

where δ is the Dirac distribution. For $f \in L^1(\mathbb{R}^2)$, the continuous ridgelet coefficient is given by

$$\mathcal{R}_f(a, b, \theta) = \int f(x)\overline{\psi}_{a,b,\theta}(x)dx. \tag{1}$$

Then any function $f \in L^1(\mathbb{R}^2) \cap L^2(\mathbb{R}^2)$ is represented as a continuous superposition of ridgelet functions

$$f(x) = \int_0^{2\pi} \int_{-\infty}^{\infty} \int_0^{\infty} R_f(a, b, \theta)\psi_{a,b,\theta}(x) \frac{da}{a^3} db \frac{d\theta}{4\pi}$$

Notice that (1) is also given by the wavelet transform of the Radon transform f:

$$\mathcal{R}_f(a, b, \theta) = \int Rf(\theta, t)a^{-1/2}\psi((t - b)/a)dt.$$

Deans found that the two-dimensional Fourier transform of f is equal to the one-dimensional Fourier transform of the Radon transform of f [13]:

$$\hat{f}(\xi \cos\theta, \xi \sin\theta) = \int Rf(\theta, t)e^{-i\xi t}dt.$$

Hence the Radon transform of f is obtained by the one-dimensional inverse Fourier transform of $\hat{f}(\xi \cos\theta, \xi \sin\theta)$ as a function of ξ.

B. Curvelet transform

Let Q denote a dyadic square $[k_1/2^s, (k_1 + 1)/2^s) \times [k_2/2^s, (k_2 + 1)/2^s)$ and let Q_s be the collection of all dyadic squares of scale s. We also let w_Q be a window near Q, obtained by dilation and translation of a single w, satisfying

$$\sum_{Q \in Q_s} w_Q^2 = 1.$$

We define multiscale ridgelets $\{w_Q T_Q \psi_{a,b,\theta} : s \geq s_0, Q \in Q_s, a > 0, b \in \mathbb{R}, \theta \in [0, 2\pi)\}$, where $T_Q f(x_1, x_2) = 2^s f(2^s x_1 - k_1, 2^s x_2 - k_2)$. Then we have the reconstruction formula

$$\begin{aligned} f &= \sum_{Q \in Q_s} f w_Q^2 \\ &= \sum_{Q \in Q_s} \\ &\int_0^{2\pi} \int_{-\infty}^{\infty} \int_0^{\infty} \langle f, w_Q T_Q \psi_{a,b,\theta} \rangle w_Q T_Q \psi_{a,b,\theta} \frac{da}{a^3} db \frac{d\theta}{4\pi} \end{aligned}$$

The curvelet transform is given by filtering and applying multiscale ridgelet transform on each bandpass filters as follows:

1) *Subband Decomposition.* The image is filtered into subbands:
$$f \to (P_0 f, \Delta_1 f, \Delta_2 f, \cdots),$$
where a filter P_0 deals with frequencies $|\xi| \leq 1$ and the bandpass filter Δ_s is concentrated near the frequencies $[2^s, 2^{2s+2}]$, for example,
$$\Delta_s = \Psi_{2s} * f, \hat{\Psi}_{2s}(\xi) = \hat{\Psi}(2^{-2s}\xi);$$
2) *Smooth Partitioning.* Each subband is smoothly windowed into "squares" of an appropriate scale
$$\Delta_s f \to (w_Q \Delta_s f)_{Q \in Q_s};$$
3) *Renormalization.* Each resulting square is renormalized to unit scale
$$g_Q = (T_Q)^{-1}(w_Q \Delta_s f), Q \in Q_s;$$
4) *Ridgelet Analysis.* Each square is analysed via the discrete ridgelet transform.

For improved visual and numerical results of the digital curvelet transform, Starck et al. presented the following discrete curvelet transform algorithm [6], [14]:

1) apply the à trous algorithm with J scales:
$$I(x, y) = C_J(x, y) + \sum_{j=1}^{J} w_j(x, y),$$
where c_J is a coarse or smooth version of original image I and w_j represents "the details of I" at scale 2^{-j};
2) set $B_1 = B_{min}$;
3) for $j = 1, \cdots, J$ do
   a) partition the subband w_j with a block size B_j and apply the digital ridgelet transform to each block;
   b) else $B_{j+1} = B_j$.

III. The image fusion method based on the curvelet transform

The following is the specific operational procedure for the proposed curvelet-based image fusion approach. While the operational procedure may be generally applied , Landsat ETM+ images are utilized as an example in order to illustrate the method.

1) The original Landsat ETM+ panchromatic and multispectral images are geometrically registered to each other.

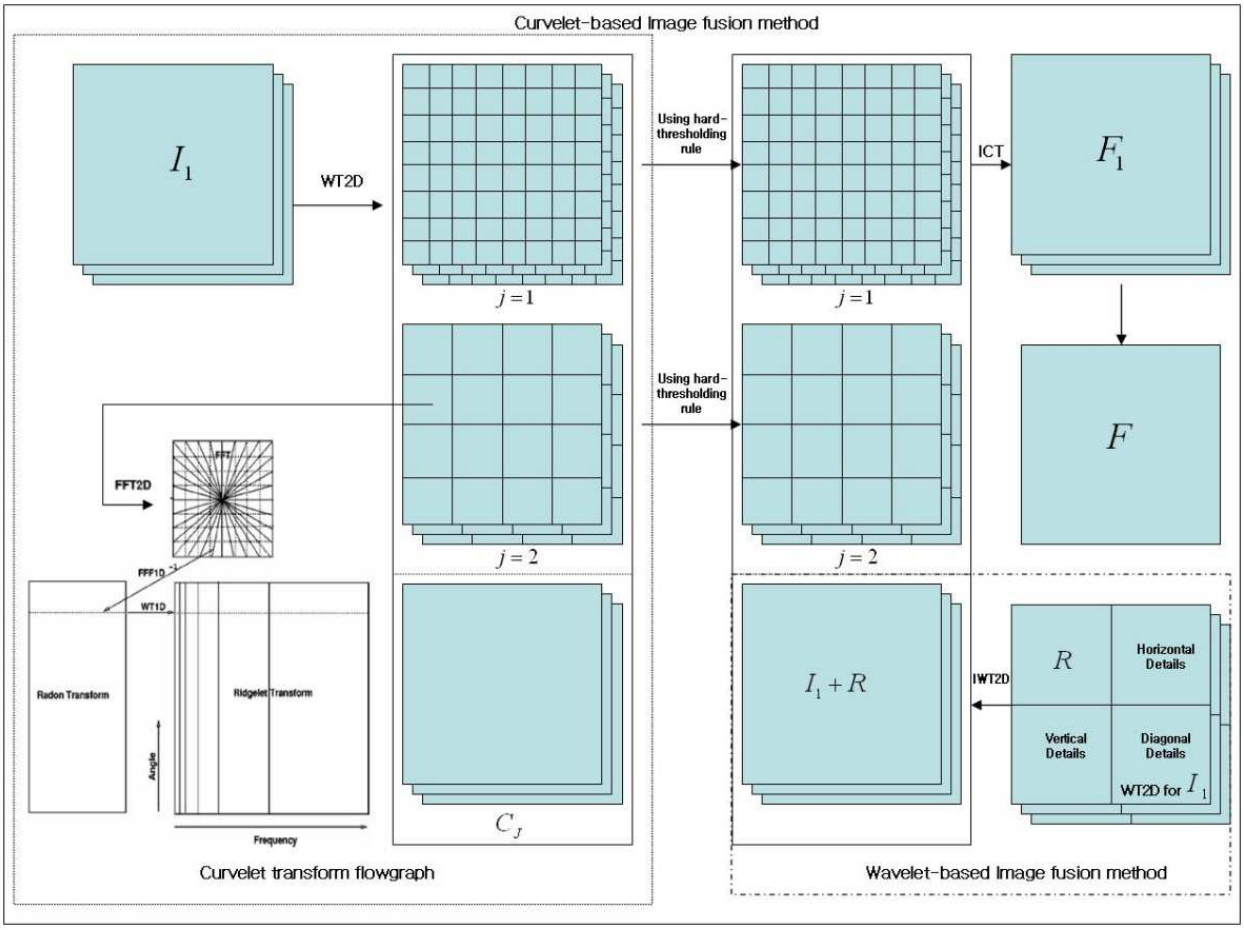

Fig. 1. Curvelet-based image fusion method.

2) Three new Landsat ETM+ panchromatic images I_1, I_2 and I_3 are produced. The histograms of these images are specified according to the histograms of the multispectral images R, G and B, respectively.
3) Using the well-known wavelet-based image fusion method, we obtain fused images $I_1 + R$, $I_2 + G$ and $I_3 + B$, respectively.
4) I_1, I_2 and I_3, which are taken from 2), are decomposed into $J + 1$ subbands, respectively, by applying "à trous" subband filtering algorithm. Each decomposed image includes C_J, which is a coarse or smooth version of the original image, and w_j, which represents "the details of I" at scale 2^{-j}.
5) Each C_J is replaced by a fused image obtained from 3). For example, (C_J for I_1) is replaced by ($I_1 + R$).
6) The ridgelet transform is then applied to each block in the decomposed I_1, I_2 and I_3, respectively.
7) Curvelet coefficients (or ridgelet coefficients) are modified using hard-thresholding rule in order to enhance edges in the fused image.
8) Inverse curvelet transforms (ICT) are carried out for I_1, I_2 and I_3, respectively. Three new images (F_1, F_2 and F_3) are then obtained, which reflect the spectral information of the original multispectral images R, G and B, and also the spatial information of the panchromatic image.
9) F_1, F_2 and F_3 are combined into a single fused image F.

In this approach, we can obtain an optimum fused image that has richer information in the spatial and spectral domains simultaneously. Therefore, we can easily find small objects in the fused image and separate them. As such, the curvelets-based image fusion method is very efficient for image fusion.

IV. EXPERIMENTAL STUDY AND ANALYSIS

A. Visual analysis

Since the wavelet transform preserves the spectral information of the original multispectral images, it has the high spectral resolution in contrast with the IHS-based fusion result, which has some colour distortion. But the wavelet-based fusion result has much less spatial information than that of the IHS-based fusion result.

To overcome this problem, we use the curvelet transform in image fusion. Since the curvelet transform is well adapted to represent panchromatic image containing edges, the curvelet-based fusion result has both high spatial and spectral resolution.

From the curvelet-based fusion result in the Landsat ETM+ image fusion presented in Figure 2, it should be noted that both

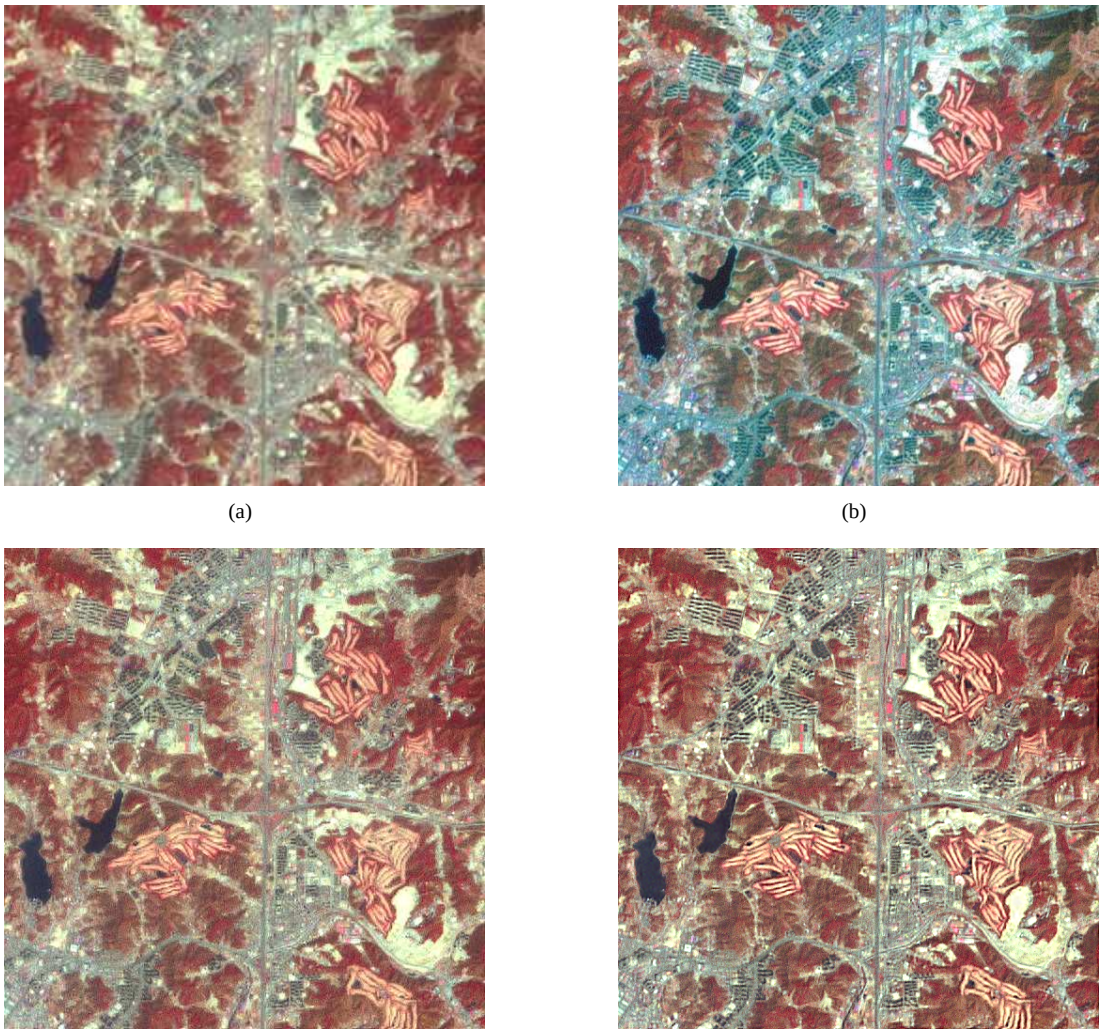

(a) (b) (c) (d)

Fig. 2. (a) Original Landsat ETM+ color image. (b) IHS-based fusion result. (c) Wavelet-based fusion result. (d) Curvelet-based fusion result.

the spatial and the spectral resolutions have been enhanced, in comparison with the original colour image. That is, the fused result contains both the structural details of the higher spatial resolution panchromatic image and the rich spectral information from the multispectral images. Moreover, compared with the fused results obtained by the wavelet and IHS, the curvelet-based fusion result has a better visual effect, such as contrast enhancement.

B. Quantitative analysis

In addition to the visual analysis, we conducted a quantitative analysis. The experimental results were analysed based on the combination entropy, the mean gradient, and the correlation coefficient, as used in [2], [15]–[17].

Table I presents a comparison of the experimental results of image fusion using the curvelet-based image fusion method, the wavelet-based image fusion method, and the IHS method in terms of combination entropy, mean gradient, and correlation coefficient.

The combination entropy of an image is defined as

$$H(f_1, f_2, f_3) = -\sum_{i=0}^{255} P_{i_1,i_2,i_3} \log_2 P_{i_1,i_2,i_3},$$

where P_{i_1,i_2,i_3} is the combination probability of the image f_1, f_2 and f_3, in which pixel values are i_1, i_2 and i_3, respectively, for the same position. The combination entropy (C.E.) represents the property of combination between images. The larger the combination entropy of an image, the richer the information contained in the image. In Table I, the combination entropy of the curvelet-based image fusion is greater than that of other methods. Thus, the curvelet-based image fusion method is superior to the wavelet and IHS methods in terms of combination entropy.

The mean gradient is defined as

$$\overline{g} = \frac{1}{MN} \sum_{i=1}^{M} \sum_{j=1}^{N} \sqrt{(\Delta I_x^2 + \Delta I_y^2)/2},$$

$$\Delta I_{x;i,j} = f(i+1, j) - f(i, j), \Delta I_{y;i,j} = f(i, j+1) - f(i, j),$$

TABLE I
A COMPARISON OF IMAGE FUSION BY THE WAVELETS, THE CURVELETS, AND IHS METHODS.

Method	C.E	M. G	C.C
Original		14.1035	-
Images	4.1497	17.9416	-
(R,G,B)		13.3928	-
Image fused		15.7327	0.8134
by IHS	2.8135	15.4414	0.9585
(F1, F2, F3)		15.0168	0.9303
Image fused		16.5891	0.9013
by Wavelet	5.8611	18.9083	0.9176
(F1, F2, F3)		17.0362	0.8941
Image fused		19.5549	0.9067
by Curvelet	5.8682	22.8330	0.9318
(F1, F2, F3)		20.9101	0.9119

where M and N are the length and width, in terms of pixel number, of an image f. The mean gradient (M.G.) reflects the contrast between the detailed variation of pattern on the image and the clarity of the image.

The correlation coefficient is defined as

$$Corr(A,B) = \frac{\sum_{m,n}(A_{mn} - \overline{A})(B_{mn} - \overline{B})}{\sqrt{(\sum_{m,n}(A_{mn} - \overline{A})^2)(\sum_{m,n}(B_{mn} - \overline{B})^2)}},$$

where $\overline{A}$ and $\overline{B}$ stand for the mean values of the corresponding data set. The correlation coefficient (C.C.) between the original and fused image shows similarity in small size structures between the original and synthetic images. In Table I, the mean gradient and the correlation coefficient of the curvelet-based image fusion method are greater than those of the wavelet-based image fusion method. Hence, we can see that the curvelet-based fusion method is better than the wavelet-based fusion method in terms of the mean gradient and correlation coefficient.

Based on the experimental results obtained from this study, the curvelet-based image fusion method is very efficient for fusing Landsat ETM+ images. This new method has yielded optimum fusion results.

V. CONCLUSION

We have presented a newly developed method based on a curvelet transform for fusing Landsat ETM+ images. In this paper, an experimental study was conducted by applying the proposed method, as well as other image fusion methods, to the fusion of Landsat ETM+ images. A comparison of the fused images from the wavelet and IHS method was made. Based on experimental results pertaining to three indicators - the combination entropy, the mean gradient, and the correlation coefficient- the proposed method provides better results, both visually and quantitatively, for remote sensing fusion. Since the curvelet transform is well adapted to represent panchromatic images containing edges and the wavelet transform preserves the spectral information of the original multispectral images, the fused image has both high spatial and spectral resolution.

ACKNOWLEDGMENT

The authors would like to express their sincere gratitude to Electronics and Telecommunications Research Institute for providing the Landsat ETM+ images for this research.

REFERENCES

[1] T. Ranchin and L. Wald, “Fusion of High Spatial and Spectral Resolution images: The ARSIS Concept and Its Implementation,” *Photogrammetric Engineering and Remote Sensing*, vol. 66, 2000, pp. 49-61.

[2] L. Wald, T. Ranchin and M. Mangolini, “Fusion of Satellite images of different spatial resolution: Assessing the quality of resulting images,” *Photogrammetric Engineering and Remote Sensing*, vol. 63, no. 6, 1997, pp. 691-699.

[3] J. Nunez, X. Otazu, O. Fors, A. Prades, V. Pala and R. Arbiol, “Multiresolution-based image fusion with addtive wavelet decomposion,” *IEEE Transactions on Geoscience and Remote sensing*, vol. 37, no. 3, 1999, pp. 1204-1211.

[4] E. J. Candès, “Harmonic analysis of neural networks,” *A ppl. Comput. Harmon. Anal.*, vol. 6, 1999, pp. 197-218.

[5] E. J. Candès and D. L. Donoho, “Curvelets- A surprisingly effective nonadaptie representation for objects with edges,” in *Curve and Surface Fitting: Saint-Malo*, A. Cohen, C.Rabut, and L.L.Schumaker, Eds. Nashville, TN: Vanderbilt Univ. ersity Press, 1999.

[6] J. L. Starck, E. J. Candès and D. L. Donoho, “The curvelet transform for image denosing,” *IEEE Trans. Image Processing*, vol. 11, 2002, pp. 670-684.

[7] J. L. Starck, E, J. Candès, and D. L. Donoho, “Gray and Color Image Contrast Enhancement by the Curvelet Transform,” *IEEE Trans. Image Processing*, vol. 12, no. 6, 2003, pp. 706-717.

[8] E. J. Candès, “Ridgelets: Theory and Applications,” Ph.D. Thesis, Department od Statistics, Stanford University, Standford, CA, 1998.

[9] D. L. Donoho, “Digital ridgelet transform via rectopolar coordinate transform,” Stanford Univ., Stanford, CA, Tech. Rep, 1998.

[10] D. L. Donoho, “Orthonormal ridgelets and linear singularities,” *SIAM J. Math Anal.*, vol. 31, no. 5, 2003, pp. 1062-1099.

[11] I. Daubechies, “Ten Lectures on Wavelets,” CBMS-NSF series in Applied Mathematics, SIAM, Philadelphia, 1992.

[12] P. G. Lemarié and Y. Meyer, “Ondelettes et bases Hilbertiennes,” *Rev. Mat. Iberoamericana*, 2, 1986, pp. 1-18.

[13] S. R. Deans, “The Radon Transform and Some of Its Application,” New York: Wiley, 1983.

[14] J. L. Starck, F. Murtagh and R. Bijaoui, ”Image Processing and Data Analysis: The Multiscale Approach,” Cambridge, U.K.: Cambridge Univ. Press, 1998.

[15] J. Li and Z. J .Liu, “Data fusion for remote sensing imagery based on feature,” *China Journal of Remote Sensing*, vol. 2, no. 2, 1998, pp. 103-107 (in Chinese with abstract in English).

[16] W. Z. Shi, C. Q. Zhu, C. Y. Zhu and X. M. Yang, “Multi-Band Wavelet for Fusing SPOT Panchromatic and Multispectral Images,” *Photogrammetric Engineering and Remote Sensing*, vol. 69, no. 5, 2003, pp . 513-520.

[17] J. B. Sun, J. L. Liu and J. Li, “Multi-source remote sensing image data fusion,” *China Journal of Remote Sensing*, vol. 2, no. 1, 1998, pp. 47-50 (in Chinese with abstract in English).